Article

Journal of
Nanoscience and Nanotechnology
Vol. 15, 8813–8819, 2015
www.aspbs.com/jnn

Julolidine—Based Organic Dyes with Neutral and Anion Anchoring Groups for Dye-Sensitized Solar Cells

Le Quoc Bao, Nguyen Thi Hai, Chi Hwan Lee, Suresh Thogiti*, and Jae Hong Kim*

Department of Chemical Engineering, Yeungnam University, Gyeongsan, Gyeongsangbuk-do, 712-749, Republic of Korea

Two simple organic dyes (**J1** and **J2**) containing julolidine as the electron donor were synthesized. The simple structure of julolidine attached to the cyanoacetic acid group formed two compounds (anion and neutral forms of E-CCVJ), which showed two different efficiencies when applied to dye-sensitized solar cells (DSSCs). Overall conversion efficiencies of 0.91% and 1.21% were obtained for DSSCs based on the cyanoacetic acid (**J1**) and cyanoacetate (**J2**) derived dyes, respectively. Compared to the cyanoacetic acid terminated dye, the current density, open circuit voltage and conversion efficiency of the solar cells based on cyanoacetate dye were increased by approximately 24%, 8% and 32%, respectively. The electrochemical impedance analysis showed that the better charge transfer of TiO_2 (e^-) and electron lifetime (τ_e) for **J2** dye as compared with **J1**. The power conversion efficiency was found to be quite sensitive to small structural changes to the anchoring moiety.

Keywords: Dye Sensitized Solar Cells, Julolidine Sensitizers, Nanocrystalline TiO_2, UV-Vis Absorption.

1. INTRODUCTION

Since O'Regan and Grätzel introduced Dye-Sensitized Solar Cells (DSSCs) in 1991, they have attracted considerable interest in the scientific community.[1–3] DSSCs have also attracted the attention of chemists, physics, and engineers around the world owing to their construction and operation, their high incident-solar-light-to-electricity conversion efficiency and low cost of production.[4–6] To increase the performance of DSSCs, it is very important to create highly efficient sensitizers. The ideal sensitizer for a DSSC should have a high molar extinction coefficient and absorb solar radiation strongly with absorption bands preferably covering the broad ranges of wavelengths across visible to near infrared regions. In addition, the sensitizer should anchor strongly to the semiconductor surface to achieve good electronic communication and inject electrons efficiently into the conduction band of TiO_2.

Recently, DSSC based on a Zn-porphyrin complex were reported to have a power conversion efficiency (PCE) of 13%[7] and those with the ruthenium complex dyes also reached 11%[8–12] under standard AM 1.5G sunlight. On the other hand, the use of rare and expensive metals in dye synthesis has limited their commercial applicability. Metal-free organic dyes as alternative sensitizers have attracted considerable attention because of their potential advantages, such as control of the structure of organic compounds, the use of inexpensive and environmentally benign resources, high molar extinction coefficient, and facile synthesis.[13–16] To date, a myriad organic dyes, such as triphenyl amine,[17–19] coumarne,[20–22] cyanine,[23, 24] perylene,[25–27] indoline,[28–31] fluorine,[32–34] carbazole,[35–37] phenothiazine,[38–40] phenoxazine,[41–43] tetrahydroquinoline,[44–47] and ullazine,[48–50] have been evaluated as sensitizers and the highest efficiency cells have achieved comparable PCEs (>10%) to those with metal-based dyes.[51–54] For example, an impressively high cell efficiency of 12.8% has also been achieved using a metal-free sensitizer.[15] On the other hand, a better fundamental understanding is needed to design a new, efficient and stable organic sensitizers for future devices. For instance, the adsorption mode influences the electronics states of the dye/TiO_2 interface, such as the conduction band position of the TiO_2 surface, the photo-absorption spectra of the dye itself[55–57] and the electron injection efficiency.[58] Conventionally, the deprotonated anchor is regarded as being more stable than the protonated anchor.[59] Therefore,

---

*Authors to whom correspondence should be addressed.

1533-4880/2015/15/8813/007 doi:10.1166/jnn.2015.11536

investigation of the protonation/deprotonation of dye carboxyl anchor is still important.

9-(2-carboxy-2-cyanovinyl)julolidine (CCVJ) is a member of a class of molecules commonly known as "molecular rotor." This material was first introduced by Sawada in 1992 as one of a series of fluorophores with greater water solubility to study the association phenomena in biological systems.[60] Several julolidine dyes have been used as sensitizers in DSSCs because of their large π-conjugated system and better electron donating property.[61–65] In this study, anion and neutral derivatives of cyanoacetic acid were introduced to the simple julolidine based dyes for anchoring in an attempt to achieve better anchoring of the cyanoacetate anion and increase photovoltaic performance through potential electrostatic interactions with the semiconductor (TiO_2) surface. Therefore, two new organic dyes **J1** (neutral) and **J2** (anion), were designed and applied to DSSCs and compared with standard **N719**[12] dye under similar fabrication and measurement conditions. To explain the photovoltaic properties of the ionic dye system in DSSCs, the UV-Vis spectra of the two compounds, current density–voltage characteristics, impedance analysis, and the incident photo-to-current conversion efficiencies were studied.

2. EXPERIMENTAL DETAILS

2.1. Equipment and Measurements

All ^1H NMR spectra were recorded on a Varian Mercury NMR 300 MHz spectrometer using $CDCl_3$ and DMSO-d_6, which were both purchased from Alfa Aesar Company. The chemical shifts were referenced to TMS. The absorption spectra were recorded on an Agilent 8453 UV-Vis spectrophotometer. The active areas of the dye-absorbed TiO_2 films were estimated using a digital microscope camera with image-analysis-software (Moticam 1000). The photovoltaic I–V characteristics of the prepared DSSCs were measured under 1 sunlight intensity (100 mW cm^{-2}, AM1.5), which was verified with an AIST-calibrated Si-solar cell (PEC-L11, Peccell Technologies, Inc., City, State, Country). The incident monochromatic photon-to-current efficiencies (IPCEs) were plotted as a function of the light wavelength using an IPCE measurement instrument (PEC-S20, Peccell Technologies, Inc.).

2.2. Synthesis of Sensitizers

Julolidine was purchased from TCI and stored at low temperatures. N, N-dimethylformamide (DMF), cyanoacrylic acid and piperidine were obtained from Sigma-Aldrich and used as received. Phosphoryl chloride ($POCl_3$) and other solvents, such as dichloromethane (DCM), chloroform ($CHCl_3$) and diethyl ether (Et_2O), were purchased from Alfa-Aesar and used as received. All reactions were performed under an inert gas (N_2) and the products were stored in the dark.

2.2.1. Synthesis of 9-Julolidinecarboxaldehyde (1)

Julolidine (0.5 g, 2.89 mmol), DMF (0.255 g, 3.49 mmol) and $POCl_3$ (0.535 g, 3.49 mmol) were dissolved in DCM (15 mL) and the mixture was stirred at room temperature for 4 h under an inert argon atmosphere. The solution's color turned green and the degree of advancement was followed by TLC. The solution was treated with aq. NaOH (2 M) and the crude product then was extracted with Et_2O. After two aqueous washings, the organic phase was dried on $MgSO_4$, filtered and concentrated under vacuum. The product was then purified on column chromatography using 40%–50% Et_2O: Hexane was used as the eluent to give 0.48 g (83.08%) (the reaction yield was up to 92% when 1.5 g julolidine was used as starting material) of a light yellow solid product.^1H NMR (300 MHz, $CDCl_3$):$\delta = 9.597$ (s, 1 H), 7.29 (s, 1 H), 3.308 (t, $J =$ 5.7 Hz, 4 H), 2.787 (t, $J = 6.2$, 4 H), 2.002–1.92 (m, $J =$ 6.3, 4 H).

2.2.2. Synthesis of 9-(2-carboxy-2-cyanovinyl) Julolidine (CCVJ)

9-Julolidinecarboxaldehyde (0.5 g, 2.49 mmol), cyanoacetic acid (0.3 g, 3.53 mmol), and piperidine (0.3 g, 3.52 mmol) were dissolved in 15 mL AcCN and stirred for 5 h at 60 °C. The reaction progress was monitored by TLC. Subsequently, water was added to the solution and the crude product was extracted with CH_2Cl_2. After two aqueous washings, the organic phase dried on Na_2SO_4, filtered and concentrated under vacuum. The product was then purified by column chromatography using 5% MeOH: CH_2Cl_2 and 0.05 g (7.5%) of a solid product (CCVJ) was obtained. Finally, the crude product was recrystallized with MeOH to produce two compounds, which were called **J1** (neutral CCVJ) and **J2** (anion CCVJ), respectively. **J1** and **J2** were tested using the ^1H NMR method. **J1**—^1H NMR (300 MHz, DMSO): $\delta = 7.849$ (s, 1 H), 7.487 (s, 2 H), 3.337 (t, $J = 5.7$ Hz, 4 H), 2.690 (t, $J = 6.0$ Hz, 4 H), 1.907 (m, $J = 5.7$ Hz, 4 H). **J2**—^1H NMR (300 MHz, DMSO): $\delta = 7.688$ (s, 1 H), 7.326 (s, 2 H), 3.265 (t, $J =$ 5.7 Hz, 4 H), 2.680 (t, $J = 6.0$ Hz, 4 H), 1.880 (m, $J =$ 6.0 Hz, 4 H).

2.3. Assembly and Characterization of DSSCs

The transparent conducting glass substrates were cleaned sequentially with ethanol, DI water and acetone with ultrasonication. The TiO_2 pastes were prepared using ethyl cellulose (Aldrich), Lauric acid (Fluka, City, State, Country), and terpineol (Aldrich). The TiO_2 particles used were *ca*. 20–30 nm in diameter. The prepared TiO_2 paste was doctor-bladed onto pre-cleaned glass substrates, followed by drying at 70 °C for 30 min and 30 min calcination at 500 °C. The scattering layer consisting of rutile TiO_2 particles (250 nm in a size) was deposited on mesoporous TiO_2 films. These layers were dipped into an aqueous solution of $TiCl_4$ (0.04 M) at 70 °C for 30 min. The sensitizers

(**J1** and **J2**) were dissolved in DMF (0.3 mM) at room temperature and stirred for 24 h. The TiO_2 layers were immersed in the solutions for 24 h.

The Pt counter electrodes were prepared by thermal reduction of the films dip-coated in H_2PtCl_6 (7.0 mM) in 2-propanol at 400 °C for 20 min. The dye-adsorbed TiO_2 and Pt counter electrodes were sandwiched between 60 μm-thick Surlyn (Dupont 1702), which was used as a bonding agent and spacer. Through a pre-punched hole on the Pt counter electrode, a liquid electrolyte (I^-/I_3^- redox couple) was then introduced and finally sealed. The active area of the dye-adsorbed TiO_2 films was estimated using a digital microscope camera with image-analysis-software (Moticam 1000).

3. RESULTS AND DISCUSSION

3.1. Synthesis

Julolidine and cyanoacetic acid were chosen as the donor and acceptor moieties for the two metal-free organic sensitizers, **J1** and **J2**. Although there are a few reports on the role of julolidine as a metal-free organic sensitizer, it was used to synthesize the simplest julolidine sensitizers with a small change in their anchoring moiety for DSSC applications.

The synthesis of two new organic sensitizers was carried out according to Scheme 1. Julolidine was subjected to Vilsmeier–Haack formylation in the presence of dichloromethane. The crude reaction mixture after work up was separated by column chromatography to obtain pure 9-julolidinecarboxaldehyde (**1**) in good yield. Knoevenagel condensation of intermediate **1** with cyanoacetic acid in the presence of piperidine for 5 h at 60 °C yielded a crude dye, which was purified by recrystallization using MeOH to give the sensitizers, **J1** and **J2**. 9-Julolidinecarboxaldehyde (**1**) and the sensitizers (**J1** and **J2**) were characterized by ^{1}HNMR spectroscopy.

3.2. Optical Properties

Figure 1 shows the UV-Visible absorption spectra of **J1** and **J2** dyes in DMF. From the spectra, at lower concentrations, the absorption peaks for **J1** and **J2** appeared to be the same (at approximately 375 nm). By increasing the concentration of both **J1** and **J2**, **J1** showed a red shift in absorption. Further increasing the concentration resulted in a clear absorption peak at 441 nm. In contrast, the solution of **J2** in DMF, showed no such change in the absorption spectra with changing concentration. The relative ratio of the peaks depends not only on the concentration, but also on the solution temperature. By increasing

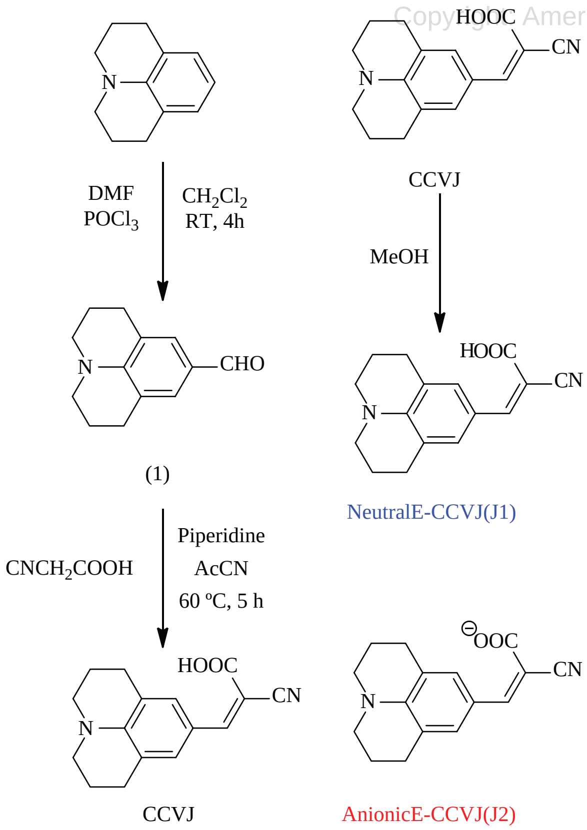

Scheme 1. Synthesis of the CCVJ sensitizers **J1** and **J2**.

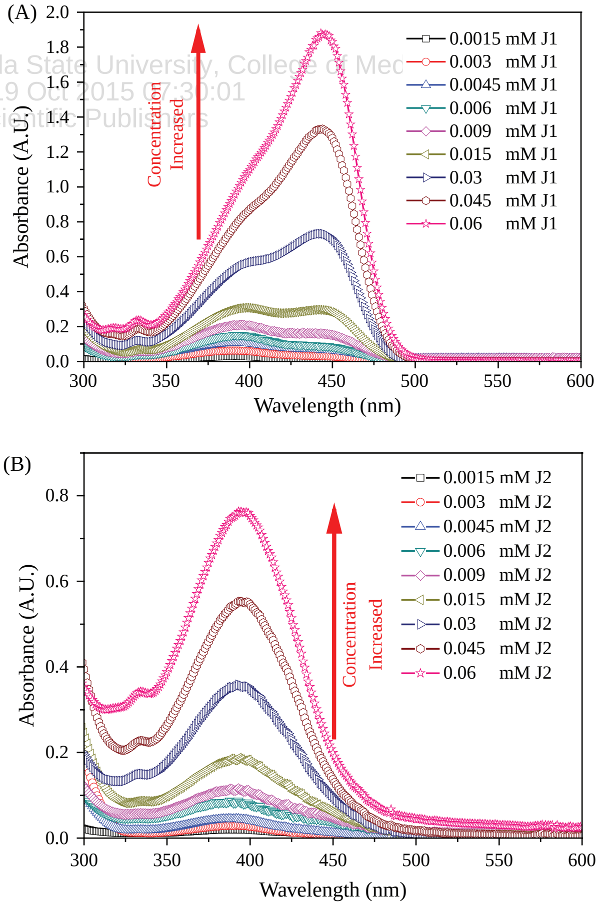

Figure 1. UV-Vis absorption spectra of **J1** (A) and **J2** (B) in DMF at various concentrations.

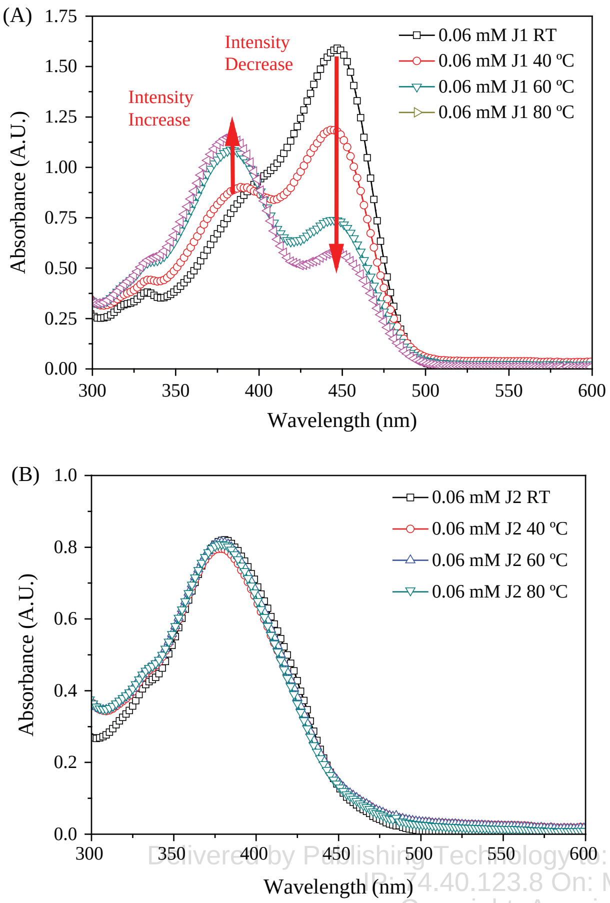

Figure 2. Effect of temperature on UV-Vis spectra of **J1** (0.06 mM) in DMF: Upon increasing the temperature to 80 °C (A) and Effect of temperature on UV-Vis spectra of **J2** (0.06 mM) in DMF: Upon increasing the temperature to 80 °C (B).

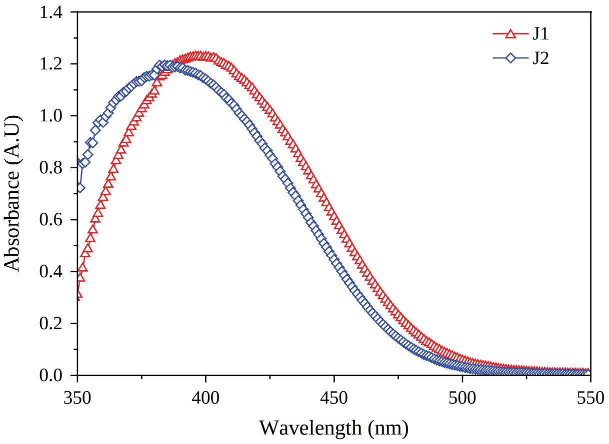

Figure 3. UV-Vis spectra of **J1** and **J2** attached on TiO_2 film.

the temperature of the solution of **J1** in DMF, the absorption intensity began decreasing at 441 nm and increasing at 375 nm (Fig. 2(A)). These concentration- and temperature dependent behaviors of the **J1** sensitizer suggest a red shift in the absorbance after forming aggregates. In contrast, no change in the absorption spectrum was observed with increasing temperature of the **J2** solution in DMF (Fig. 2(B)).

The absorption spectra of the spin-coated thin films of **J1** and **J2** were recorded to investigate the interactions between the molecules in the solid state (Fig. 3). Generally, the absorption maxima of the organic dyes on the TiO_2 films would change because of the different effects of the deprotonation in the adsorption process and the aggregation state of dyes on TiO_2 films. In our case, a red shift between the organic sensitizer **J2** on the TiO_2 films and in solution was observed, which might be due to the J-type aggregation. In addition, the absorption spectrum of the **J2** sensitizer anchored onto the TiO_2 film showed a slightly broad profile compared to the solution spectrum, which was beneficial for light harvesting. The broadening and red shift in the spectrum of **J2** might be due to the presence of anion groups in the molecule because this functional group may increase the likelihood of favorable electrostatic interactions with the TiO_2 surface. The interactions between the carboxylate group and the surfaceTi^{4+} ions may lead to increased delocalization of the π^* orbital of the conjugated framework. The energy of the π^* level is decreased by this delocalization, which explains the red shift in the absorption spectra. The blue-shift of the absorption spectra of dye **J1** on TiO_2 compared to solution can be attributed to deprotonation of the carboxylic acid group and/or the formation of H aggregates on the TiO_2 surface.[46,66] From the absorption studies, the julolidine-based sensitizer containing a carboxylate anion as the anchoring group may be a good sensitizer compared to other sensitizers with a cyanoacetic acid anchoring group for DSSC applications.

3.3. Photovoltaic Properties

The photovoltaic properties of the solar cells constructed from **J1** and **J2** of the E-CCVJ TiO_2 electrode were measured under simulated AM 1.5 irradiation (100 mW cm^{-2}). The open-circuit photovoltage (V_{OC}), short-circuit photocurrent density (J_{SC}), fill factor (FF), and solar-to-electricity conversion efficiencies (η) were compared with those of **N719** and are listed in Table I. Figures 4 and 5 show the incident photo-to-current conversion efficiencies (IPCE) and current density–voltage (J–V) characteristics of the devices based on the two dyes, respectively. The DSSC coated with **J2** exhibited a much better IPCE of approximately 50% at approximately 450 nm in the solar response range. For the **J1** based cell, the IPCE reached its maximum of 40% at 450 nm. **J2** produced a higher IPCE value between 350 nm and 550 nm than the **J1** dye. On the

Table I. Photovoltaic parameters of the DSSCs based on **J1**, **J2** and standard **N719**.

Sensitizer	J_{SC} (mA/cm^2)	V_{OC} (V)	FF (%)	η (%)
N719	16.84	0.7299	61.62	7.575
J1	3.186	0.4214	67.76	0.91
J2	3.955	0.4575	67.08	1.21

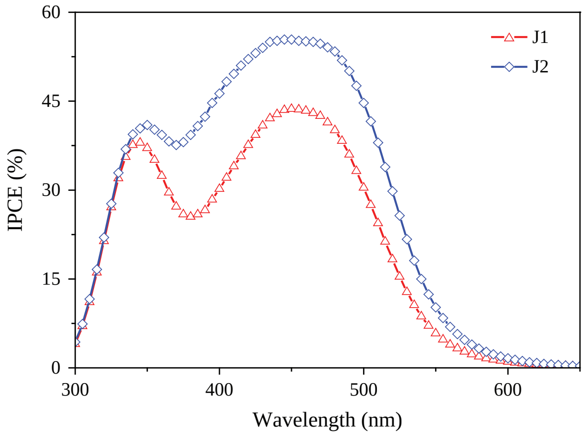

Figure 4. IPCE curves of the DSSCs using **J1** and **J2**.

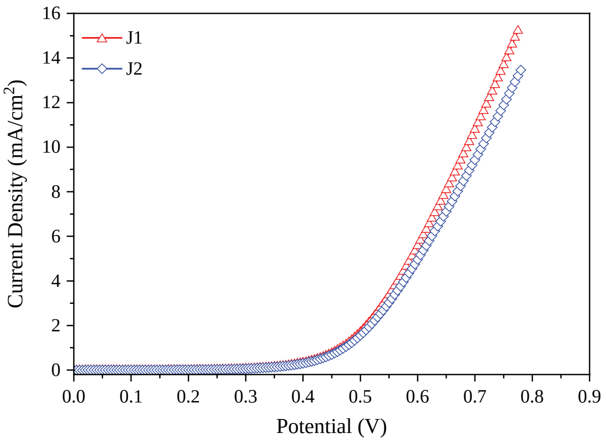

Figure 6. *J–V* curves obtained with DSSCs based on **J1** and **J2** dyes under dark conditions.

other hand, the IPCE values for **J1** and **J2** decreased significantly after 500 nm, which was attributed to a decrease in the light harvesting property. The **J1** sensitized solar cell showed a J_{SC} of 3.18 mA^{-2}, V_{OC} of 0.421 V and *FF* of 67.76%, corresponding to a η of 0.91%, whereas the **J2** sensitized cell yielded a J_{SC} of 3.95 mA^{-2}, a V_{OC} of 0.457 V and a *FF* of 67.08%, corresponding to a η of 1.21%. Under similar test conditions, the **N719** dye gave a referenced η value of 7.57%.

The observed J_{SC} values of the DSSCs based on **J2** were higher than those based on **J1** under one sun illumination, which is in agreement with the improved IPCE spectrum. This suggests that the cyanoacetate anion-anchoring dye **J2** with a broad and red-shifted spectrum could inject more electrons effectively into the TiO_2 conduction band. On the other hand, the cyanoacetic acid anchoring dye **J1** decreased the IPCE of the dye. Therefore, the cells based on the dye with the cyanoacetic acid anchoring group showed narrower IPCEs than those based on the cyanoacetate anion-anchoring dye, resulting in lower J_{SC} values. Therefore, the cyanoacetate anion as an anchoring moiety provides an opportunity for organic dyes to exhibit high energy conversion performance.

A dark current test, which is a technique for testing the capability of charge recombination, was conducted and the results are shown in Figure 6. The onset for **J1** was slightly lower than **J2**. This suggests that the back-electron-transfer process corresponding to a reaction between the conducting-band electrons in the TiO_2 and I_3^- in the electrolyte under dark conditions occurs more easily in the DSSCs based on neutral E-CCVJ (**J1**) after adsorbing on the TiO_2 layer. Compared to **J1**, the J_{SC} and V_{OC} of the solar cells based on **J2** are increased about 24% and 8%, respectively. The higher J_{SC} and V_{OC} for the DSSCs of **J2** lead to a higher efficiency. Finally, an increase in η of approximately 32% was obtained from **J1** to **J2**. A likely reason for this may be the better electrostatic interactions of the anion form of E-CCVJ with the TiO_2 surface, which ultimately gives **J2** better conversion efficiency than **J1**.

To further understand the FTO/TiO_2/dye interface, we performed electrochemical impedance spectroscopy

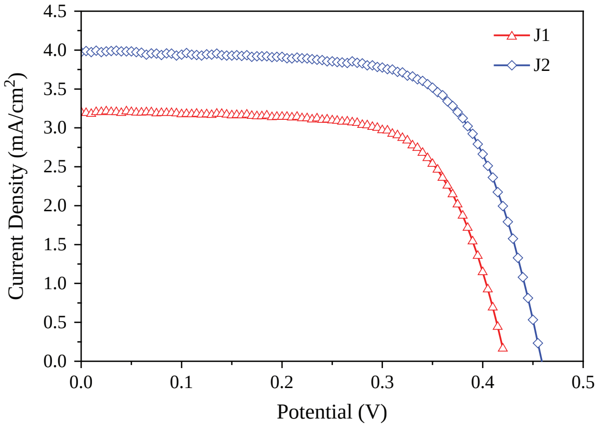

Figure 5. Current density–voltage (*J–V*) characteristics of the DSSCs from **J1** and **J2** under the illumination of simulated solar light (AM 1.5, 100 mW cm^{-2}).

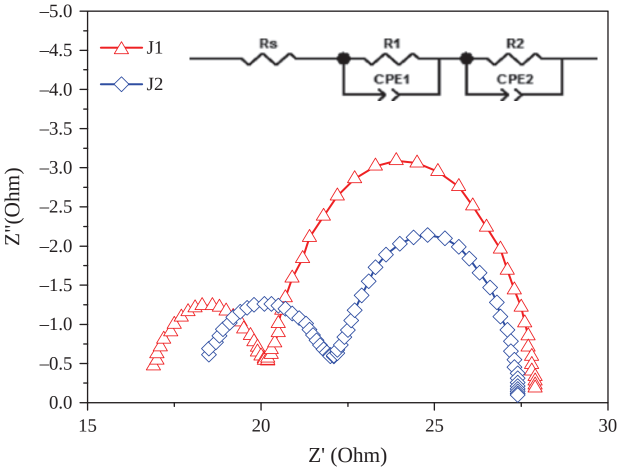

Figure 7. Impedance spectra (Nyquist plots) based on **J1** and **J2** under AM1.5 light conditions.

Table II. Electrochemical parameters of DSSCs.

Sample	$R_S(\Omega)$	$R_{CE}(\Omega)$	$R_{CT}(\Omega)$	τ_e
$\mathbf{J_1}$	16.45	3.587	7.727	12.63
$\mathbf{J_2}$	17.98	4.23	5.249	15.92

studies (EIS) since this technique has been a useful tool to estimate charge transfer resistance and to know the dye regeneration efficiency. Figure 7 shows EIS results for DSSCs comprised of FTO/TiO_2/**J1** and FTO/TiO_2/**J2** electrodes under illuminated. The smaller and larger semicircles in the Nyquist plots were attributed to the charge transfer at the counter electrode and the working electrode interface, respectively. R_S is the series resistance, R_{CT} is the electron transfer resistance between the TiO_2 film and electrolyte and R_{CE} is the resistance of electron transport in the counter electrode. The fitting results are summarized in Table II. The Nyquist plots (Fig. 7) showed the radius of the semicircle corresponding to the working electrode to be higher for FTO/TiO_2/**J1** compared to FTO/TiO_2/**J2**. The charge transfer resistance (R_{CT}) for FTO/TiO_2/**J1** and FTO/TiO_2/**J2** were 7.72 and 5.24 Ω, respectively (Table II). The decrease in charge transfer resistance for FTO/TiO_2/**J2** compared to FTO/TiO_2/**J1** can be attributed to the better performance, i.e., photoregeneration of FTO/TiO_2/**J2** is much efficient, a result that agrees well with the cell efficiency shown in Figures 4 and 5 (Table I).

The recombination rate caused by the backward charge transfer was estimated using the Bode-phase spectra for the DSSCs, as shown in Figure 8. The electron lifetimes were calculated and shown in Table II. The frequency of the characteristic peak in the Bode phase plot increased in the order of **J2** < **J1**. A lower characteristic frequency in the Bode phase plot means a slower charge recombination rate and higher V_{OC}. As the reciprocal of the characteristic frequency is correlated with electron lifetime (τ_e), electron lifetime increased in the order of **J1** < **J2**. This sequence of the electron lifetime calculated from the Bode phase plot also indicated increasing resistance to recombination. The lower R_{CT} and longer τ_e observed for cyanoacetate anion dye **J2** compared to cyanoacetic acid dye **J1** indicates a more effective suppression of the back reaction of the injected electron with the I_3^- in the electrolyte, reflecting in the improvement of the J_{SC} and V_{OC}, yielding a substantially enhanced power conversion efficiency.

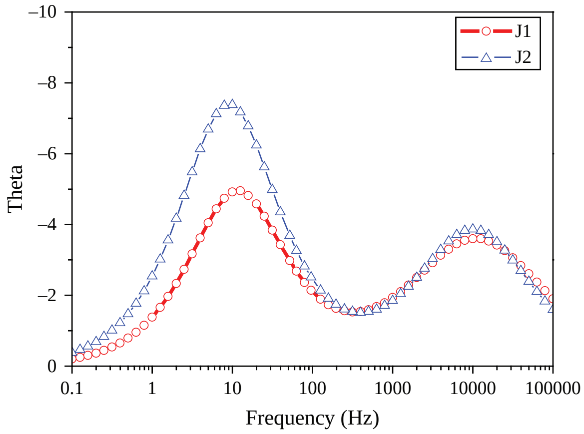

Figure 8. Impedance spectra (Bode plots) based on **J1** and **J2**.

4. CONCLUSION

Sensitizers based on julolidine with the simplest structure were synthesized and used on DSSCs to test their efficiencies. The simple structure of julolidine attached to the cyanoacrylic acid group formed two compounds (anion and neutral forms of E-CCVJ), which gave two different efficiencies when applied to DSSCs. The **J2** dye with the cyanoacetate anion as the anchoring group showed redshift in the absorption band on the TiO_2 film compared to **J1** dye with a cyanoacetic acid as the anchoring group. The simple structure of the donor-anchoring CCVJ showed reasonable results (0.91% for **J1** and 1.21% for **J2**). Sensitizer **J2** showed a 32% improvement in the overall power conversion efficiency compared to **J1**, which could be due to its better electrostatic interactions with the TiO_2 surface. The EIS analysis of the DSSCs shows that the charge transfer resistance (R_{CT}) is lowered and electron lifetime (τ_e) is increased for anion anchored dye; this is consistent with the results of the photocurrents and the power conversion efficiencies. The results suggest that the cyanoacetate acceptor produces DSSCs with better properties than those of the cyanoacetic acid acceptor in the julolidine dyes. This data suggests that sensitizers based on julolidine compounds could show impressive results if eligible π-bridges can be added. Research on studying this class of julolidine metal-free organic dyes towards achieving higher solar to electricity conversion efficiencies is currently underway.

Acknowledgment: This research was supported by Basic Science Research Program through the National Research Foundation of Korea (NRF) funded by the Ministry of Education, Science and Technology (grant number: 2012014395).

References and Notes

1. B. O'Regan and M. Grätzel, *Nature* 353, 737 **(1991)**.
2. A. Hagfeldt, G. Boschloo, L. Sun, L. Kloo, and H. Pettersson, *Chem. Rev.* 110, 6595 **(2010)**.
3. S. F. Zhang, X. D. Yang, Y. Numata, and L. Y. Han, *Energ. Environ. Sci.* 6, 1443 **(2013)**.
4. L. Han, A. Islam, H. Chen, C. Malapaka, B. Chiranjeevi, S. Zhang, X. Yang, and M. Yanagida, *Energ. Environ. Sci.* 5, 6057 **(2012)**.
5. A. Yella, H.-W. Lee, H. N. Tsao, C. Yi, A. K. Chandiran, M. K. Nazeeruddin, E. W.-G. Diau, C.-Y. Yeh, S. M. Zakeeruddin, and M. Grätzel, *Science* 2011, 629 **(2011)**.
6. Y. Ooyama and Y. Harima, *Chem. Phys. Chem.* 13, 4032 **(2012)**.
7. S. Mathew, A. Yella, P. Gao, R. Humphrey-Baker, B. F. E. Curchod, N. Ashari-Astani, I. Tavernelli, U. Rothlisberger, M. K. Nazeeruddin, and M. Grätzel, *Nat. Chem.* 6, 242 **(2014)**.

8. F. Gao, Y. Wang, J. Zhang, D. Shi, M. Wang, R. Humphry-Baker, P. Wang, S. M. Zakeeruddin, and M. Grätzel, *Chem. Commun.* 44, 2635 (**2008**).

9. C. Y. Chen, M. K. Wang, J. Y. Li, N. Pootrakulchote, L. Alibabaei, C. Ngoc-Le, J. D. Decoppet, J. H. Tsai, C. Grätzel, C. G. Wu, S. M. Zakeeruddin, and M. Grätzel, *ACS Nano* 3, 3103 (**2009**).

10. F. F. Gao, Y. Wang, D. Shi, J. Zhang, M. K. Wang, X. Y. Jing, R. Humphry-Baker, P. Wang, S. M. Zakeeruddin, and M. Grätzel, *J. Am. Chem. Soc.* 130, 10720 (**2008**).

11. Q. Yu, Y. Wang, Z. Yi, N. Zu, J. Zhang, M. Zhang, and P. Wang, *ACS Nano* 4, 6032 (**2010**).

12. M. K. Nazeeruddin, F. D. Angelis, S. Fantacci, A. Selloni, G. Viscardi, P. Liska, S. Ito, B. Takeru, and M. Grätzel, *J. Am. Chem. Soc.* 127, 16835 (**2005**).

13. M. Grätzel, *Accounts. Chem. Res.* 42, 1788 (**2009**).

14. Z. Ning, Y. Fu, and H. Tian, *Energ. Environ. Sci.* 3, 1170 (**2010**).

15. M. Zhang, Y. Wang, M. Xu, W. Ma, R. Li, and P. Wang, *Energ. Environ. Sci.* 6, 2944 (**2013**).

16. J. Y. Mao, N. N. He, Z. J. Ning, Q. Zhang, F. L. Guo, L. Chen, W. J. Wu, J. L. Hua, and H. Tian, *Angew. Chem. Int. Edit.* 51, 9873 (**2013**).

17. H. Li, Y. Hou, Y. Yang, R. Tang, J. Chen, H. Wang, H. Han, T. Peng, Q. Li, and Z. Li, *ACS Appl. Mater. Inter.* 5, 12469 (**2013**).

18. Z. Wang, M. Liang, L. Wang, Y. Hao, C. Wang, Z. Sun, and S. Xue, *Chem. Commun.* 49, 5748 (**2013**).

19. J. Chen and M. Liang, *Chem. Soc. Rev.* 42, 3453 (**2013**).

20. K. Hara, K. Sayama, H. Arakawa, Y. Ohga, A. Shinpo, S. Suga, and H. Arakawa, *Chem. Commun.* 6, 569 (**2001**).

21. Z.-S. Wang, Y. Cui, K. Hara, Y. Dan-Oh, C. Kasada, and A. Shinpo, *Adv. Mater.* 19, 1138 (**2007**).

22. S. E. Koops, P. R. F. Barnes, B. C. O'Regan, and J. R. Durrant, *J. Phys. Chem. C* 114, 8054 (**2010**).

23. Y.-S. Chen, C. Li, Z.-H. Zeng, W.-B. Wang, X.-S. Wang, and B.-W. Zhang, *J. Mater. Chem.* 15, 1654 (**2005**).

24. L. Beverina, R. Ruffo, C. M. Mari, G. A. Pagani, M. Sassi, F. De Angelis, S. Fantacci, J.-H. Yum, M. Grätzel, and M. K. Nazeeruddin, *Chem. Sus. Chem.* 2, 621 (**2009**).

25. C. Li, J. H. Yum, S. J. Moon, A. Herrmann, F. Eickemeyer, N. Pschirer, P. Erk, J. Schöneboom, K. Müllen, M. Grätzel, and M. K. Nazeeruddin, *Chem. Sus. Chem.* 1, 615 (**2008**).

26. S. Mathew and H. J. Imahori, *J. Mater. Chem.* 21, 7166 (**2011**).

27. A. A. Vasilev, K. De Mey, I. Asselberghs, K. Clays, B. Champagne, S. E. Angelova, M. I. Spassova, C. Li, and K. Müllen, *J. Phys. Chem. C* 116, 22711 (**2012**).

28. T. Horiuchi, H. Miura, K. Sumioka, and S. J. Uchida, *J. Am. Chem. Soc.* 126, 12218 (**2004**).

29. S. Ito, H. Miura, S. Uchida, M. Takata, K. Sumioka, P. Liska, P. Comte, P. Pechy, and M. Grätzel, *Chem. Commun.* 41, 5194 (**2008**).

30. B. Liu, W. Li, B. Wang, X. Li, Q. Liu, Y. Naruta, and W. Zhu, *J. Power Sources* 234, 139 (**2013**).

31. T. Horiuchi, H. Miura, and S. Uchida, *Chem. Commun.* 24, 3036 (**2003**).

32. L.-Y. Lin, C.-P. Lee, M.-H. Yeh, A. Baheti, R. Vittal, K. R. J. Thomas, and K.-C. J. Ho, *J. Power Sources* 215, 122 (**2012**).

33. H. Qin, S. Wenger, M. Xu, F. Gao, X. Jing, P. Wang, S. M. Zakeeruddin, and M. Grätzel, *J. Am. Chem. Soc.* 130, 9202 (**2008**).

34. H. Choi, C. Baik, S. Kang, J. Ko, M. S. Kang, M. K. Nazeeruddin, and M. Grätzel, *Angew. Chem. Int. Edit.* 47, 327 (**2008**).

35. K. S. V. Gupta, T. Suresh, S. P. Singh, A. Islam, L. Han, and M. Chandrasekharam, *Org. Electron.* 15, 266 (**2014**).

36. A. Venkateswararao, K. R. J. Thomas, C. P. Lee, C. T. Li, and K. C. Ho, *ACS Appl. Mater. Inter.* 6, 2528 (**2014**).

37. Y. Uemura, T. N. Murakami, and N. Koumura, *J. Phys. Chem. C* 118, 16749 (**2014**).

38. Y. Hua, S. Chang, D. Huang, X. Zhou, X. Zhu, J. Zhao, T. Chen, W. Y. Wong, and W. K. Wong, *Chem. Mater.* 25, 2146 (**2013**).

39. S. Agrawal, M. Pastore, G. Marotta, M. A. Reddy, M. Chandrasekharam, and F. D. Angelis, *J. Phys. Chem. C* 117, 9613 (**2013**).

40. H. Tian, X. Yang, R. Chen, Y. Pan, L. Li, A. Hagfeldt, and L. Sun, *Chem. Commun.* 36, 3741 (**2007**).

41. H. Tian, X. Yang, J. Cong, R. Chen, J. Liu, Y. Hao, A. Hagfeldt, and L. Sun, *Chem. Commun.* 41, 6288 (**2009**).

42. M. Karlsson, L. Yang, M. K. Karlsson, L. Sun, G. Boschloo, and A. Hagfeldt, *J. Photoch. Photobio. A* 239, 55 (**2012**).

43. H. Tan, C. Pan, G. Wang, Y. Wu, Y. Zhang, Y. Zou, G. Yu, and M. Zhang, *Org. Electron.* 14, 2795 (**2013**).

44. M. Cheng, X. Yang, J. Li, F. Zhang, and L. Sun, *Chem. Sus. Chem.* 6, 70 (**2013**).

45. Y. Hao, X. Yang, J. Cong, H. Tian, A. Hagfeldt, and L. Sun, *Chem. Commun.* 27, 4031 (**2009**).

46. R. Chen, X. Yang, H. Tian, and L. J. Sun, *J. Photoch. Photobio. A* 189, 295 (**2007**).

47. R. Chen, X. Yang, H. Tian, X. Wang, A. Hagfeldt, and L. Sun, *Chem. Mater.* 19, 4007 (**2007**).

48. J. Feng, Y. Jiao, W. Ma, M. K. Nazeeruddin, M. Grätzel, and S. Meng, *J. Phys. Chem. C* 117, 3772 (**2013**).

49. J. H. Delcamp, A. Yella, T. W. Holcombe, M. K. Nazeeruddin, and M. Grätzel, *Angew. Chem. Int. Edit.* 52, 376 (**2013**).

50. A. Dualeh, R. H. Baker, J. H. Delcamp, M. K. Nazeeruddin, and M. Grätzel, *Adv. Energy Mater.* 3, 496 (**2013**).

51. W. Zeng, Y. Cao, Y. Bai, Y. Wang, Y. Shi, M. Zhang, F. Wang, C. Pan, and P. Wang, *Chem. Mater.* 22, 1915 (**2010**).

52. A. Mishra, M. K. R. Fischer, and P. Bäuerle, *Angew. Chem. Int. Edit.* 48, 2474 (**2009**).

53. K. Kakiage, Y. Aoyama, T. Yano, T. Otsuka, T. Kyomen, M. Unno, and M. Hanay, *Chem. Commun.* 50, 6379 (**2014**).

54. J. Yang, P. Ganesan, J. Teuscher, T. Moehl, Y. J. Kim, C. Yi, P. Comte, K. Pei, T. W. Holcombe, M. K. Nazeeruddin, J. Hua, S. M. Zakeeruddin, H. Tian, and M. Grätzel, *J. Am. Chem. Soc.* 136, 5722 (**2014**).

55. F. De Angelis, S. Fantacci, A. Selloni, M. K. Nazeeruddin, and M. Grätzel, *J. Am. Chem. Soc.* 129, 14156 (**2007**).

56. F. De Angelis, S. Fantacci, A. Selloni, M. Grätzel, and M. K. Nazeeruddin, *Nano Lett.* 7, 3189 (**2007**).

57. F. De Angelis, S. Fantacci, A. Selloni, M. Grätzel, and M. K. Nazeeruddin, *Nanotechnology* 19, 424002 (**2008**).

58. C. Bauer, G. Boschloo, E. Mukhtar, and A. Hagfeldt, *J. Phys. Chem. B* 106, 12693 (**2002**).

59. K. Sodeyama, M. Sumita, C. O. Rourke, U. Terranova, A. Islam, L. Han, D. R. Bowler, and Y. Tateyama, *J. Phys. Chem. Lett.* 3, 472 (**2012**).

60. C. Rumble, K. Rich, G. He, and M. Maroncelli, *J. Phys. Chem. A* 116, 10786 (**2012**).

61. H. Choi, J. K. Lee, K. H. Song, K. Song, S. O. Kang, and J. Ko, *Tetrahedron* 63, 1553 (**2007**).

62. Q. Feng, X. Lu, G. Zhou, and Z.-S. Wang, *Phys. Chem. Chem. Phys.* 14, 7993 (**2012**).

63. G. Wu, F. Kong, J. Li, W. Chen, X. Fang, C. Zhang, Q. Chen, X. Zhang, and S. Dai, *Dyes. Pigments* 99, 653 (**2013**).

64. G. Wu, F. Kong, J. Li, X. Fang, Y. Li, S. Dai, Q. Chen, and X. Zhang, *J. Power Sources* 243, 131 (**2013**).

65. G. Wu, F. Kong, J. Li, W. Chen, C. Zhang, Q. Chen, X. Zhang, and S. Dai, *Synthetic. Met.* 180, 9 (**2013**).

66. L.-Y. Lin, C.-H. Tsai, K.-T. Wong, T.-W. Huang, L. Hsieh, S.-H. Liu, H.-W. Lin, C.-C. Wu, S.-H. Chou, H. Chen, and A.-I. Tsai, *J. Org. Chem.* 75, 4778 (**2010**).

Received: 19 July 2014. Accepted: 22 December 2014.